



Post-Irradiation Mechanical Properties Prediction of Al 6070 of MTR-Fuel Bundle for Cutting Process



Antonio Gogo Hutagaol^{1,2}, Imam Hidayat¹, Maman Kartaman Ajiriyanto², Supaat Zakaria³

¹Department of Mechanical Engineering, Faculty of Engineering, Universitas Mercu Buana, Indonesia

²Research Center for Nuclear Fuel Cycle and Radioactive Waste Technology, National Research and Innovation Agency (BRIN), Indonesia

³Department of Mechanical Engineering, Politeknik Ungku Omar, Malaysia

Abstract

The Al 6070 is the side plate material of the MTR-fuel plate bundle. These post-irradiation mechanical properties will be used in the side plate cutting process to obtain certain plates from the MTR-fuel plate bundle. This activity is part of a series of post-irradiation test processes from the MTR-fuel plate bundle in order to determine its performance. After testing in the form of a bundle (assembly), then continued testing of certain plates from the bundle. Disassembly of the plate is carried out by cutting along the two side plates (aluminum alloy) that clamp the plate. The mechanical properties of the workpiece material are important factors that affect the conditions of the machining (cutting) process. Prediction of post-irradiation mechanical properties was carried out using the change percentage of before and after irradiation of other aluminum alloys. The prediction carried out with the Si transmutation as the dominant one affects the post-irradiation mechanical properties changes in aluminum alloys. The change percentage added the mechanical properties of the pre-irradiated side plate material of the MTR-fuel plate bundle. Pre-irradiation testing of the Al 6070, namely chemical composition tests, pre-irradiation mechanical properties tests, including hardness tests (micro), and tensile tests (max stress, yield stress, and % elongation). Prediction of changes in mechanical properties of side plate material (aluminum alloy, Al 6070) before irradiation, compared to after irradiation is: hardness value from 98.51 to 127 ($gf/\mu m^2$), tensile strength from 265.371 to 398 (N/mm^2), the yield strength from 204.2 to 306 N/mm^2 .

This is an open access article under the [CC BY-NC](https://creativecommons.org/licenses/by-nc/4.0/) license



Keywords:

Mechanical Properties;
MTR-Fuel Plate;
Nuclear Research Reactor;
Post Irradiation Examination;

Article History:

Received: September 27, 2021

Revised: December 6, 2021

Accepted: December 26, 2021

Published: June 15, 2022

Corresponding Author:

Antonio Gogo Hutagaol,
Department of Mechanical
Engineering, Faculty of
Engineering, Universitas Mercu
Buana, Indonesia,
Email:
gogo_hutagaol@yahoo.com

INTRODUCTION

In nuclear fuel research and development activities, the fuel prototype that is produced needs to examine in the reactor core (irradiation) for a certain time and a certain burnup level reached. After leaving the reactor core, nuclear fuel was placed in a storage pool for 101 days to reduce the radiation level and transferred to a post-irradiation examination facility. The examination was carried out in order to determine the performance of the fuel through a series of

tests, both the Non-Destructive Test (NDT) and Destructive Test (DT). The examination data obtained was evaluated to determine its performance and in order to obtain a license to use the nuclear fuel from the authorized institution.

The examinations were carried out on the plate-type nuclear fuel of the Material Testing Reactor (MTR), which consisted of 21 plates, as presented in [Figure 1](#) and [Figure 2](#). After testing in the form of a bundle (assembly), then continued testing of certain plates from the bundle. The

process of disassembling the plate from the bundle structure must be carried out to obtain this particular plate. Disassembly of the plate is carried out by cutting along the two side plates (aluminum alloy) that clamp the plate.

The cutting method of the side plate to obtain the desired plate has been determined by using a CNC-Router machine. Furthermore, it is necessary to know the mechanical properties of the side plate material of the fuel bundle that will be cut and whether there are changes after irradiation, which of course, can affect the cutting process. This study aims to predict changes in the mechanical properties of the side plate material (aluminum alloy) after irradiation compared to before irradiation.

The mechanical properties of the workpiece material are important factors that affect the machining conditions. Regarding low cutting forces, low values of hardness and tensile strength usually provide better machinability [1]. The side plate is the post-irradiated condition. Therefore, it is necessary to know the mechanical properties of the side plate material (aluminum alloys) after irradiation (post-radiation). Because the experimental process (primary data) takes a long time, it is carried out using secondary data.

During the use of fuel (MTR-fuel plate) in the reactor core, a process of neutron irradiation occurs. In a thermal neutron environment, aluminum atoms are converted to silicon, and their fraction is proportional to the thermal neutron flux. The location of transmutation-produced Si deposits in the microstructure will have a major impact on the mechanical properties of the alloy. The transmuted Si will precipitate as Si elemental particles, which are uniformly distributed in the matrix and associated with voids [2][3]. The damage caused by precipitation of transmutation Si was found to be the dominant mechanism affecting the fracture toughness properties of irradiated 5xxx and 6xxx series Al alloys at high thermal fluence values [4]. Si transmutation is the dominant influence on the post-irradiation mechanical properties change, the percentage change in mechanical properties of other

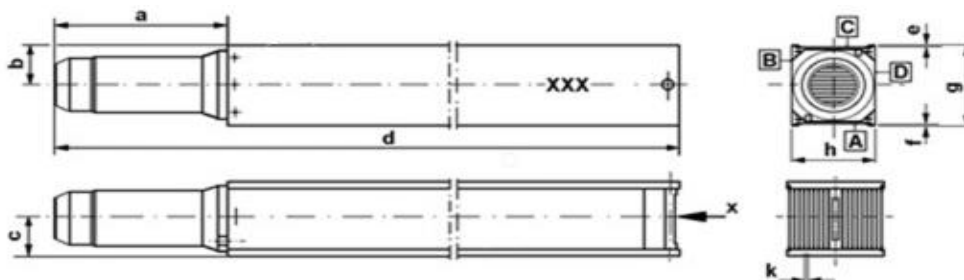
aluminum alloys between pre-irradiation and post-irradiation mechanical properties of the side plate material.

MATERIAL AND METHODS

Cutting Process Requirements

Three plates were removed from the MTR fuel bundle structure, namely two from the edge and one from the middle, and tested to represent the performance of one MTR fuel bundle. Plates with a thickness of 1.3 mm and a distance between plates of 2.55 mm. In the process of taking the plate, by making a groove cut with a width of 5 mm just above the desired plate so that it does not interfere with the adjacent plate. The cut grooves on the side plate are 5 mm deep (0.5 mm thicker than the side plate so fuel meat is still safe) and 630 mm long. A Precision for the cutting process is required as well as precise positioning of the MTR-fuel bundle on the workbench of the cutting tool. Thus, the axis of motion of the tool (cutting tool) is parallel to the axis of the MTR-fuel bundle on the workbench of the cutting tool, especially the long axis of the bundle. The cutting process is carried out inside the hot cell and controlled from outside the hot cell due to the very high radiation from the MTR fuel (post-irradiation).

- The height of the workpiece placed on the workbench of the cutting machine from the hot cell floor is a maximum of 40 cm. With this height, it is easy for the operator to monitor the cutting process from outside the hot cell through the lead glass window.
- The cutting process does not use coolant. The end of the suction hose from the vacuum cleaner that is used can be brought closer to the cutting process, which functions as a chip cleaner and can also function as a cooler.
- Components of the cutting machine made of non-metallic materials must be sufficiently resistant to the radiation present, and if necessary additional adequate radiation protective cover should be provided. The faster the time for the cutting process, the less radiation exposure received.



a 145 mm; d 868 mm; b 40 mm; c 38 mm; g 80 mm; h 76 mm

Figure 1. MTR-fuel plate bundle [5]

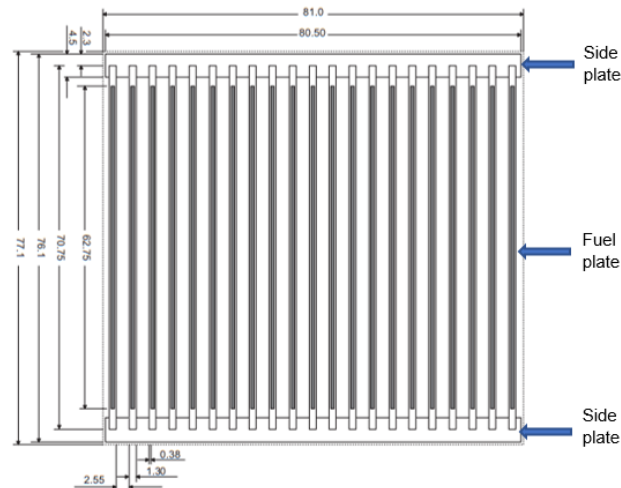


Figure 2. Cross-section of the MTR-fuel plate bundle, view X [6]

Material Machinability

Material machinability is the ease with which metallic materials can be a machine that allows the removal of the material from the cutting process with a satisfactory result and at a low cost. Material machinability requires a small cutting force, can be cut quickly, easily get a good finish, and use fewer tools. Improving the performance of material often reduces its machinability. This is a challenge in itself, to find a way to improve the engine's capabilities without sacrificing performance.

Machining capability is difficult to predict because machining has many variables. The two factors are the material condition of the workpiece and the physical properties of the material. The condition of the material includes eight factors: microstructure, grain size, heat treatment, chemical composition, fabrication, hardness, yield strength, and tensile strength. Physical properties such as modulus of elasticity, thermal conductivity, thermal expansion, and work hardening. Other important factors are operating conditions, tool geometry and material, and machining process parameters.

There are several criteria for material machinability evaluation, and the most frequently used ones are tool life (influencing the machining time and production costs), cutting forces (influencing energy consumption), cutting temperatures (influencing tool wear), and machined surface quality and chip shape. Based on these criteria, better material machinability is due to longer cutting tool life, higher productivity (the amount of removed chip), better-machined surface quality, lower cutting forces, lower cutting temperatures, and more favorable chip shapes, as long as they have been achieved under the same conditions [1][7].

Tensile strength and hardness are typical material properties influencing the main cutting

force. There is, of course, a set of other material properties, like the microstructure, crystal grains size and shape, type and amount of impurities, and the like, which also exert influence on the main cutting force [1]. Suggests a relation between yield and Vickers hardness: $HV = 2.7 \sigma_y$. The ratio between shear strength and tensile strength for ductile materials is $\tau_{Sh} = 0.6 \sigma_y$ [8].

The shearing of metal takes place while machining and major mechanical energy is converted into heat energy due to the formation of the chip. This temperature causes an adverse effect on tool and workpiece i.e., high tool wear, failure of the tool, inadequate surface integrity and lower tool life [9]. While Stability is significantly affected when the dynamic characteristics of the cutting tool are rather similar to those of the workpiece [10]. The cutting speed and the feed on the particle size depend on the workpiece material. The critical cutting speed appears to be widely influenced by the workpiece material, and not by the machining processes. It seems that the critical cutting speed depends significantly only on the workpiece material, and not on the machining processes, the tool geometry or the heat treatment [11].

Aluminum alloys are lightweight metals with a variety of attractive mechanical and thermal properties and are malleable metals in machining processes. Aluminum alloy as a material with a high level of machinability, when compared to other light metal families such as titanium and magnesium alloys. This high machinability, can be determined for a particular application by various criteria, such as tool life, surface finish, chip evacuation, material removal rate and machine tool power. This indicates that chemical composition, structural defects, and alloying elements significantly affect machinability. Thus,

with a similar chemical composition, the machinability of the alloy can be improved by different treatments. Heat treatment, which increases hardness, reduces the tendency of the built-up edge (BUE) during machining. In the case of dry machining, the main problems encountered are BUE at low cutting speeds and stickiness at high cutting speeds. Therefore, a special tool geometry is required. High levels of Magnesium (Mg) can increase the cutting force at the same level of hardness. Cutting force is one of several parameters considered for an overall assessment of the machinability of a metal alloy, including tool life, surface finish, cutting energy and chip forming mode [11].

Irradiation and Mechanical Properties

The presence of Si in the aluminum structure increases the tensile strength, decreases the ductility, and causes swelling. It can be concluded that the accumulation of ²⁸Si precipitates causes the strengthening of the aluminum alloy. The decrease in ductility and increase in tensile strength is caused by the conversion of aluminum to silicon [2].

The resulting contribution of displacement damage to irradiation hardening and embrittlement remains almost constant above the irradiation dose levels at which the dislocation density reaches the saturation value. Since then, the Si transmuted produced played a dominant role in contributing to the irradiation hardening of Al alloys [3].

Method

The material used as the workpiece for the cutting process is Al 6070, the material of the side plate. Prediction of post-irradiation mechanical properties, carried out by characterization and testing of chemical and mechanical properties of pre-irradiation first. Characterization and tests carried out are chemical composition tests and mechanical properties, including hardness and tensile tests (max stress, yield stress, and % elongation).

Chemical composition test using Mobile Spectrometer (Belec Spektrometrie Opto-Elektronik), hardness test using microhardness Tester LM 800At and tensile test using Shimadzu SCG-5kNA, which is capable of up to 20 kN.

The test samples used (as received) were three pieces of side plate material with a thickness of 4.5 mm, consisting of:

- two pieces with a size of 92 x 150 mm, to be used as tensile test specimens of 6 (six) pieces, according to ASTM E8/E8M [12], namely subsize specimens as presented in Figure 3.

- 1 piece with a size of 25 x 80 mm, as a test specimen for chemical composition and microhardness with an indenter size of about 45 x 45 m.
- Yield stress is obtained by the offset method as shown in Figure 4 by drawing a straight line (0.2% strain) parallel to the elastic line until it intersects at the plastic line (starts to bend) [12].

The percentage elongation (% elongation) is obtained by calculation based on the percentage change in length. Lf is the distance between the gauge marks after the specimen is damaged, as presented in Figure 5. While:

$$\% \text{ Elongation} = \frac{L_f - L_0}{L_0} \times 100 \quad [13] \quad (1)$$



Figure 3. The test samples (as received)

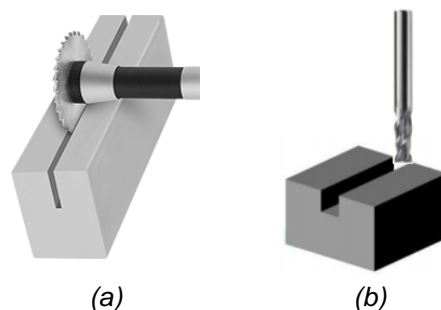


Figure 4. (a) Slitting saw blade and (b) slotting End mill



Figure 5. Specimens after tensile test

Prediction of Mechanical Properties

Prediction of the mechanical properties of the post-irradiated side plate material, especially the value of its hardness and tensile strength, using the results of post-irradiation tests of other aluminum alloys. Si transmutation is the dominant influence on changes in the mechanical properties of aluminum alloys after irradiation. Therefore, it is necessary to know the chemical composition, hardness, and tensile strength of the side plate material (pre-irradiation). Then the percentage change in mechanical properties of other aluminum alloys after irradiation compared to pre-irradiation is known from other research activities (secondary data). The percentage change is used to predict the mechanical properties of the side plate material after irradiation.

RESULTS AND DISCUSSION

Cutting Process

The requirements for the cutting process require a CNC milling. A CNC Milling Machine is a machine-operated cutting tool that is programmed and managed by a Computer Numerical Control (CNC) system to remove/cut material from the workpiece accurately, using Computer-Aided Design (CAD) software. With the requirements for the height of the workpiece from the hot cell floor of 30 cm to 40 cm, the CNC milling chosen is a CNC router type with three axes (X, Y, and Z). A CNC router has a similar concept to a CNC milling machine. The cutting tool path is controlled by CNC.

With the function of making a cutting line with a depth of 5 mm, a width of 5 mm, and a length of 630 mm, there are two types of cutting tools, namely an end mill with a diameter of 5 mm or a slitting saw blade with a certain diameter, with a thickness of 5 mm. The two cutting tools are mounted on the spindle on the vertical axis (Z-axis) of the CNC router. These machines are equipped with a spindle and three linear axes for positioning or moving the part machined.

The general principle for a CNC Milling Machine is that the part is machined and clamped on the machine table. The part can be clamped directly on the table or held in place by a vice or fixture. The shaft/spindle (moving part), including the attached cutting tool, is positioned vertically or horizontally. In this configuration, the tool can reach various X-Y-Z positions to start the cutting process.

Prediction of mechanical properties

Measurement of chemical composition by portable Spectrometer for Metal Analysis and the chemical composition (concentration in %) in accordance with Aluminum 6070-T4

(<http://www.matweb.com>), the results are presented in Table 1. The hardness Vickers of Aluminum 6070-T4 is 101 HV, converted from Brinell Hardness value. Furthermore, the side plate material is called Al 6070.

Microhardness of Al 6070

Hardness test using microhardness Tester LM 800AT (Vickers microhardness), which was carried out at 6 (six) positions. The complete test results are presented in Table 2 (load of 100 gF) and have an average hardness value of 98.51 HV.

Tensile Strength and Microhardness

The dimensions of the tensile test specimen are in accordance with ASTM E8/E8M sub-size specimen [12], with a thickness of 4.5 mm, as many as 5 (five) specimens (C, D, E, F, and G). Tensile test equipment used Shimadzu SCG-5kNACAP.

In preparation for the test, the transducer force was replaced with a capacity of 10 kN, with a capacity of 10 kN, and it is known that the structure of the Shimadzu SCG-5kNA tensile tester is capable of up to 20 kN. Tensile test results data of 5 specimens are presented in Table 3 and in Figure 6.

Prediction of the hardness value of aluminum alloy after irradiation refers to the results of the U_3Si_2/Al plate cladding hardness test results, density 2.96 and 4.8 (gU/cm^3) post-irradiation as listed in Table 4 and Table 5 [13]. The clad material is AlMg2. The hardness of the post-irradiated sample was higher than that of the pre-irradiated sample. The average hardness of the pre-irradiated sample was 42.03 HV at a load of 100 gF, while the average hardness of the post-irradiated sample was 60.98 HV as shown in Table 4.

Table 1. Side plate chemical composition and Al 6070-T4 chemical composition

No.	Element	Concentration (%)
1	Al	94.5 – 98
2	Mg	0.5 – 1.2
3	Si	1.0 – 1.7
4	Mn	0.4 – 1.0
5	Fe	<= 0.5

Table 2. Microhardness of Al 6070 plate

Position	d1 (μm)	d2 (μm)	d (μm)	HV ($gF/\mu m^2$)	HV ($gF/\mu m^2$)
1	41.81	43.82	42.82	100.15	
2	42.01	42.17	42.09	103.63	
3	42.79	42.78	42.79	100.29	
4	42.89	43.15	43.02	99.20	98.51
5	44.77	44.08	44.43	93.02	
6	43.92	44.10	44.01	94.78	

Table 3. Tensile test results of Al 6070

Specimen	Max force (N)	Max Stress (N/mm ²)	Yield Stress 0.2% (N/mm ²)	% Elongation
C	7225.61	276.843	210	16
D	6980.36	264.708	195	8
E	7058.75	265.866	211	8
F	6545.72	251.227	197	12
G	7024.41	268.210	208	14
Avg.	6966.97	265.371	204.2	11.6

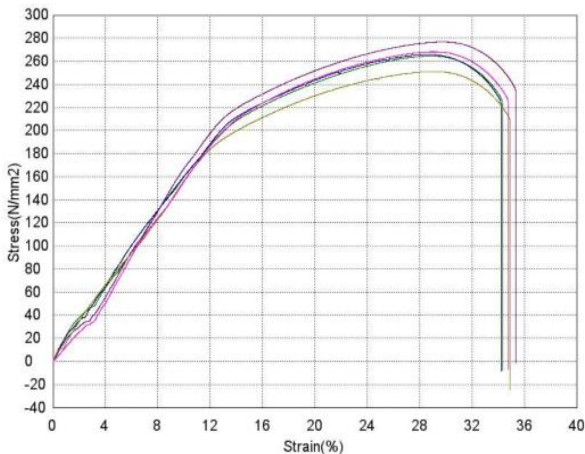


Figure 6. Graph of tensile test results for pre-irradiated specimens of side plate materials of MTR-fuel plate

The results of the hardness test for U₃Si₂/Al samples with a density of 4.8 gU/cm³ after irradiation are shown in Table 4. The average hardness value of AlMg₂ for fuel cladding of U₃Si₂/Al with a density of 4.8 gU/cm³ after irradiation was 58.28 HV as listed in Table 5. When compared with the pre-irradiation hardness value, the percentage increase in the hardness value of AlMg₂ post-irradiation (2.96 gU/cm³) is 30.6%.

The average percentage increase in the value of post-irradiation hardness is 29%. The increase in the hardness value in the post-irradiated sample is caused by the hardening mechanism due to neutron irradiation, namely the transmutation of some of the Al elements into Si, which then forms precipitates that can increase the hardness and mechanical strength. The result of the microhardness test of pre-irradiated Al 6070 was 98.51 (gf/μm²).

The percentage increase in the hardness value after AlMg₂ irradiation for a density of 4.8 gU/cm³ is 27.4% of the microhardness test of pre-irradiated Al 6070 was 98.51 (gf/μm²). The percentage increase in the hardness value after AlMg₂ irradiation for a density of 4.8 gU/cm³ is 27.4%. Prediction of hardness value after irradiation of side plate material (Al 6070) using a percentage of 29%, which is 127 (gf/μm²).

Table 4. The hardness of nuclear fuel plate cladding (U₃Si₂/Al with a density of 2.96 gU/cm³) after irradiation [14]

Position	Load gF	d1 (μm)	d2 (μm)	dr (μm)	HV (gf/μm ²)	HV (gf/μm ²)
Top	100	54.91	53.02	53.96	63.68	63.48
		54.69	53.63	54.16	63.22	
		53.77	54.28	54.03	63.53	
Middle	100	54.39	52.05	53.22	65.48	65.42
		53.87	52.65	53.26	65.37	
		54.31	52.17	53.24	65.41	
Bottom	100	60.41	56.56	58.49	54.21	54.05
		61.13	56.43	58.78	53.67	
		60.9	56.03	58.46	54.26	

Table 5. The hardness of fuel plate cladding (U₃Si₂/Al with a density of 4.8 gU/cm³) after irradiation [14]

Position	Load gF	d1 (μm)	d2 (μm)	dr (μm)	HV (gf/μm ²)	HV (gf/μm ²)
Middle	100	55.67	54.01	54.84	61.65	62.23
		54.76	54.28	54.52	62.39	
		55.17	53.63	54.4	62.66	
T-M	100	58.09	57.74	57.91	55.29	56.10
		57.3	56.05	56.68	57.73	
		58.06	57.77	57.91	55.29	
M-B	100	55.46	58.39	56.92	57.23	56.51
		56.39	56.42	56.4	58.29	
		56.03	61.16	58.59	54.01	

Irradiated Tensile Test Prediction

In Table 3, ASTM B209 [15], for Alloy 6061 (AlMgSi) with tensile strength, 260 MPa, yield strength (0.2% offset), 220 MPa and 8% elongation. The side plate material is Al 6070 with average max stress (tensile strength) of 265.371 N/mm² (MPa), yield stress of 204.2 N/mm² (MPa), and an elongation percentage of 11.6% as listed in Table 3. With relatively similar tensile strength, yield stress, and elongation data, the post-irradiation test data that will be reviewed is Al 6061 (AlMgSi).

In the study of post-irradiated Al 6061 material, the total elongation fell from 18 to about 5%, and the UTS change ranged from 45% to 60%, compared to the unirradiated values of about 280 and 330 MPa [16].

With a change of 50%, the predicted maximum stress/UTS for the side plate material in Table 3 becomes 398 N/mm², and the yield stress is 306 N/mm². With the ratio of shear strength to 0.577 of tensile strength, the shear strength of the material is 229.6 N/mm².

Cutting Process

With the plan to use a CNC router, the cutting process is done faster. The process of disassembling the fuel element plate from the MTR-fuel plate bundle is carried out by the slotting end mill method, Figure 4(b), just above the disassembled plate, along the clamping of the plate on the side plate (Lw). The slotting end mill was chosen compared to the slitting saw blade with the consideration that the vibration is smaller.

From Figure 7, specific cutting energy (Ps) ranges from 0.75 to 2.5 GJ/m³ with a mean undeformed chip thickness of 0.021 to 0.28 mm. The undeformed chip thickness in milling is defined as the distance between two consecutive cut surfaces. The end mill is selected with a diameter of 5 mm according to the requirements for the width of the groove and 2 flutes to facilitate chip flow, and a depth of cut of 5 mm (a). The length of the cutting groove (Lw) is 630 mm.

For each metal in the tool forces study, the process temperature and geometric configuration for the feed speed from 0.01 mm to 2 mm and for the cutting speed from 50 to 300 m/min [17]. Some other things that should also be considered in planning the cutting process are not only cutting speed and feeding motion but also the fuel bundle clamping, cutting force, product smoothness, machine vibration, and workpiece vibration. Thus, the results of the analysis/ planning are not an optimal approach [18, 19, 20].

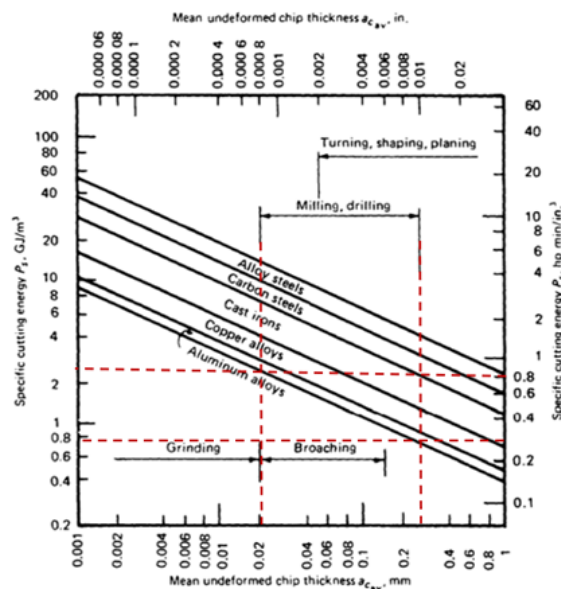


Figure 7. Approximate specific cutting energy (Ps) for various materials and operations [21]

CONCLUSION

Prediction of changes in mechanical properties of side plate material (aluminum alloy, Al 6070) after irradiation, compared to before irradiation are as follows.

1. Hardness value before irradiated is 98.51 (gf/μm²), and after irradiated is 127 (gf/μm²).
2. Tensile strength before irradiated is 265,371, and after irradiated, it is 398 N/mm².
3. Yield strength before irradiated is 204.2 N/mm², and after irradiated, it is 306 N/mm².
4. The shear strength of the material is 229.6 N/mm².

ACKNOWLEDGMENT

We thank our colleagues from the Nuclear Fuel Technology Research Center, Nuclear Energy Research Organization, and National Research and Innovation Agency (BRIN), who provided insight and expertise that greatly assisted the research of this paper.

REFERENCES

- [1] M. Sekulic, Z. Jurkovic, M. Hadzistevic, and M. Gostimirovic, "The Influence of Mechanical Properties of workpiece Material on the Main Cutting Force in Face Milling", *METALURGIJA*, vol. 49, no. 4, pp. 339-342, 2010.
- [2] V. Garric et al., "Impact of the microstructure on the swelling of aluminum alloys: Characterization and modelling bases," *Journal of Nuclear Materials*, vol. 557, 2021, doi: 10.1016/j.jnucmat.2021.153273.
- [3] IAEA-TECDOC-1871, *Material Properties Database for Irradiated Core Structural Components for Lifetime Management for Long Term Operation of Research Reactors Report of a Coordinated Research Project*, IAEA: Vienna, Austria, pp. 9-10, 2019.
- [4] M. Kolluri, "Neutron Irradiation Effects in 5xxx and 6xxx Series Aluminium Alloys: A Literature Review," *Intech*, pp. 393-411, July 2016, doi: 10.5772/63294.
- [5] NN, "Diktat of Nuclear Fuels and Post-Irradiation Tests, Re-training for IRM Operators and Supervisors," *BATAN Training Center*, 2020.
- [6] P. H. Liem, S. Amini, A. G. Hutagaol, T. M. Sembiring, "Non-destructive burnup verification by gamma-ray spectroscopy of LEU silicide fuel plates irradiated in the RSG GAS multipurpose reactor," *Annals of Nuclear Energy*, vol. 56, pp. 57-65, 2013, doi: 10.1016/j.anucene.2013.01.013.
- [7] A. R. F. Oliveira, L. R. R. da Silva, V. Baldin, M. P. C. Fonseca, R. B. Silva, and A. R. Machadoa, "Effect of tool wear on the surface

- integrity of Inconel 718 in face milling with cemented carbide tools,” *Wear*, vol. 476, 2021, doi: 10.1016/j.wear.2021.203752.
- [8] G. Genov, “Revisiting the Rule-of-Thumb Dependencies of The Shear Strength and The Hardness on Yield and the Ultimate Strengths,” *Journal of Materials Research and Technology*, 2020, doi: 10.13140/RG.2.2.24105.72807
- [9] K. Zadafiya, P. Shah, A. Shokrani, N. Khanna, “Recent advancements in nano-lubrication strategies for machining processes considering their health and environmental impacts,” *Journal of Manufacturing Processes*, vol. 68, pp. 481-511, 2021, doi: 10.1016/j.jmapro.2021.05.056
- [10] L. V. Martí'neza, J. C. Ja'uregui-Correaa, E. Rubio-Cerdaa, G. Herrera-Ruizb, A. Lozano-Guzma'nc, “Analysis of compliance between the cutting tool and the workpiece on the stability of a turning process,” *International Journal of Machine Tools & Manufacture*, vol. 48, no. 9, pp. 1054-1062, 2008, doi: 10.1016/j.ijmachtools.2007.10.016
- [11] V. Songmene, R. Khettabi, J. Kouam, and A. Djebara, “Machining and Machinability of Aluminum Alloys”, *Intech*, pp. 377-400, 2011, doi: 10.5772/14888
- [12] American Society for Testing and Materials (ASTM), *ASTM E8/E8M-16a*, Subsize Specimen, pp. 13, 2018.
- [13] E-R. Bagherian, F. Yongchang, M. Cooper, A. Amin, and F. Brian, “Effect of Atimony Addition Relative to Microstructure and Mechanical Properties of Continuous Cast Lead Alloy,” *25th Anniversary International Conference on Metallurgy and Materials (Metal 2016)*, May 2016.
- [14] M. Kartaman, E. Nurlaily, J. Carlos, Junaedi, A. Sari D.P., and E. Hermawan, “Post Irradiation Fuel Plate Cladding Hardness Test of U₃Si₂/Al, Density 2.96 and 4.8 gU/cm³”, *Proceedings of 2019 EBN Research Results*, 2019, pp. 171-180.
- [15] ASTM B209, *Standard Specification for Aluminum and Aluminum-Alloy Sheet and Plate*, 1992.
- [16] K. Farrell, and R. T. King, “Tensile Properties of Neutron-Irradiated 6061 Aluminum Alloy in Annealed and Precipitation-Hardened Conditions,” *Material Science*, pp. 440-449, 1979, doi: 10.1520/STP38180S.
- [17] C. K-M. Chen, “Analysis of the Metal Cutting Process using the Shear Plane Model,” *Master Thesis*, Montana State University, 2010.
- [18] M. Storchak, H-C. Möhring and T. Stehle, “Improving the friction model for the simulation of cutting processes,” *Tribology International*, vol. 167, 2022, doi: 10.1016/j.triboint.2021.107376.
- [19] R. S. Chandel, R. Kumar and J. Kapoor, “Sustainability aspects of machining operations: A summary of concepts,” *Materials Today: Proceeding*, vol. 50, part 5, pp. 716-727, 2022, doi: 10.1016/j.matpr.2021.04.624.
- [20] T. G. Molnar, D. Bachrathy, T. Insperger, and G. Stepan, “On process damping induced by vibration-dependency of cutting direction in milling,” *Procedia CIRP*, vol. 77, pp. 171-17, 2018, doi: 10.1016/j.procir.2018.08.270
- [21] G. Boothroyd and W. A. Knight, *Fundamentals of Machining and Machine Tools*, 3rd Edition, New York: CRC Press, 2005.